International Journal for Multidisciplinary Research (IJFMR)
E-ISSN: 2582-2160 ● Website: www.ijfmr.com ● Email: editor@ijfmr.com

Deep Learning-Based Classification of Pulmonary Diseases from Chest X-Ray Images

Burcu Oltu[1], Berna Dengiz[2], Selda Güney[3]

[1]Department of Biomedical Engineering, Baskent University, Ankara, Turkey
[2]Department of Industrial Engineering, Baskent University, Ankara, Turkey
[3]Department of Electrical and Electronics Engineering, Baskent University, Ankara, Turkey

Abstract
COVID-19, tuberculosis (TB), and pneumonia, are life-threatening diseases, that lead to death if not diagnosed or treated promptly. Chest X-rays (CXRs) are the primary imaging technique for detecting pulmonary diseases due to their ease of use, accessibility, low radiation doses, and reasonable pricing. However, interpreting CXRs is highly dependent on radiologists' experience and is prone to diagnostic errors. Therefore, a computer-aided diagnostic system may improve the detection accuracy. In this study, a deep learning-based (DL) end-to-end model is proposed for the classification of CXRs into TB, pneumonia, COVID-19, lung opacity, and healthy classes. The proposed model uses DenseNet201 as the backbone model for feature extraction and includes a squeeze-and-excitation block, and global average pooling (GAP) to highlight representative features while suppressing the redundant ones. This approach results in an average test accuracy of 98.94%, precision of 98.22%, recall of 98.03%, specificity of 99.18%, F1-score of 98.12%, and area under curve (AUC) of 0.996 for classifying five categories. This DL-based model provides objective results and performs better than existing methods in literature. Ablation studies are also conducted to show the effectiveness of the proposed method. Additionally, Grad-CAM is used to provide a visual representation of the model's decision-making process.

Keywords: Chest X-Ray, Deep Learning, Convolutional Neural Networks, Attention Mechanism, Grad-CAM

1. Introduction

Pulmonary diseases are medical conditions that impair the lungs and prevent them from working properly. According to the World Health Organization (WHO), lung diseases are a major public health problem worldwide [1]. Every year, millions of people suffer from lung diseases, and thousands die due to age, existing health problems, and late diagnosis. [1]–[3]. COVID-19, tuberculosis (TB), and pneumonia are lethal examples of pulmonary diseases that affect millions of people and put a heavy strain on both patients and healthcare systems. Since the COVID-19 outbreak in China, the global death toll has reached 6,987,222, with cases still rising. The 2023 WHO report states that TB was the second leading cause of death from a single infectious agent in 2022, following COVID-19. Pneumonia is also highly dangerous, causing rapid lung deterioration and suffocation affecting 7% of the population each year [4]. Although these diseases are deadly and contagious, the mortality rates caused by these diseases can be reduced with early diagnosis and treatment. Despite their severity, early diagnosis and treatment

can reduce the death rates of these diseases. Therefore, an early and effective diagnosis is crucial [1], [5].

Three-dimensional imaging techniques like computed tomography (CT), positron emission tomography (PET), and magnetic resonance imaging (MRI), can help diagnose pulmonary diseases. While these advanced techniques are effective for detecting pneumonia, they are expensive and not widely available in many parts of the world. [1], [6], [7]. In contrast, chest radiography is the most commonly used pulmonary imaging technique globally and in underdeveloped countries because it is affordable, widely available, and has low radiation levels [1], [5], [8]–[11].

Chest radiography is one of the most widely used imaging techniques worldwide because it is easy to obtain, has low radiation exposure, is non-invasive, affordable, and accessible compared to other imaging methods. It makes up at least one-third of all examinations in a typical radiology department [6]. Radiologists must accurately interpret millions of Chest X-ray (CXR) images [1]. These interpretations require significant skill, experience, and concentration [10]. However, the large number of CXRs increases the risk of misinterpretation [2], [7]. Interpreting CXRs is challenging, can lead to subjective errors, and can be time-consuming. [1], [6], [8], [12]. False positives can cause patient anxiety, require unnecessary follow-up appointments, and lead to invasive diagnostic interventions. Additionally, diseases overlooked during screening may only be detected at a severe stage, making them harder to treat [9], [10], [13].

In recent years, significant advancements in machine learning (ML) and deep learning (DL) have prompted researchers to concentrate on developing automated systems for healthcare, especially for analyzing CXRs. However, most existing systems are trained on small datasets, and focus on classifying two (COVID-19 vs. normal) or three classes (COVID-19 vs. pneumonia vs. normal), with some targeting four classes [14]–[17].

In this study, we propose an end-to-end DL network to classify four classes of pulmonary diseases and healthy CXRs. Our approach combines transfer learning, squeeze-and-excitation (SE) module, and global average pooling (GAP) to create a robust classification network. Given the importance of accurately distinguishing pulmonary diseases to determine appropriate treatment, we trained and tested our model on a large dataset of CXRs, including COVID-19, pneumonia, TB, lung opacity, and healthy cases. We evaluated the model's performance using accuracy, precision, recall, F1-score, the area under the curve (AUC), and the confusion matrix.

Our paper is organized as follows. In Section 2, a comprehensive summary of related works about classification of CXRs is given. Following this, Section 3 delineates the dataset employed and outlines our methodological approach. In Section 4 the main results of the study are provided. Section 5 engages in a detailed discussion of these findings, including a comparison with algorithms proposed in existing literature. Finally, drawn conclusions are given in Section 6.

2. Related Works

In recent years, researchers have focused on developing automated ML and DL approaches to detect pulmonary diseases, especially COVID-19, using CXRs. Although these methods are promising, they still need improvements [18]. Most of these approaches have focused on classifying COVID-19 and normal CXRs, with fewer methods classifying four or five different classes.

In 2021, Mamalakis et al. [19] proposed a deep transfer learning approach called DenResCov-19 to classify COVID-19, pneumonia, TB, and healthy CXRs. Their method combined the feature maps

obtained from DenseNet121 and ResNet50 with convolution and pooling layers to make the final decision. This approach achieved 82.9% accuracy, 69.7% sensitivity, 75.8% F1-score, and 95.1% micro-mean AUC for four-class classification.

Also in 2021, Hong et al. [20] proposed an EfficientNet-B7-based model for multi-class classification of normal, pneumonia, pneumothorax, and TB. They first pre-processed the images by cropping out non-lung areas and then used the cropped images for classification. They proposed a multi-GAP structure that extracted features from each layer of EfficientNet-B7, compressed them with GAP, and combined them. This method achieved an average accuracy of 96.10%, an average sensitivity of 92.20%, and an average specificity of 97.40% for the four-class classification.

Kim et al. [21] proposed an end-to-end transfer learning-based DL approach for classifying four types of CXRs (normal, pneumonia, pneumothorax, and TB) They used EfficientNet v2, pre-trained on ImageNet, as the base model and added GAP, dropout, and dense layers. They achieved a maximum accuracy of 82.20%, sensitivity of 81.40%, and specificity of 94.48%.

Bhandari et al. [3] developed a lightweight convolutional neural network (CNN) for classifying COVID-19, pneumonia, TB, and normal CXRs. Their model included five convolution layers, max-pooling, dropout, smoothing, and dense layers. They achieved an overall validation accuracy of 94.54%, demonstrating good results for classifying pneumonia diseases. They also used various explainable AI algorithms like SHAP, LIME, and Grad-CAM to evaluate the results.

Iqbal et al. [22] proposed a new methodology to distinguish normal, TB, pneumonia and COVID-19 CXRs. Their proposed methodology combines a segmentation network (TB-UNet) based on an extended fusion block and an attention block, and a classification network (TB-DenseNet) combining five dual convolution blocks and DenseNet169 for precise classification. Using this network, they achieved 95.10% accuracy, 95.67% precision, 95.10% sensitivity, and 95.38 F1 score, respectively, and showed that they achieved better performance than state-of-the-art methods.

Sultana et al. [23] developed a CNN architecture consisting of three convolutional layers, followed by max pooling, flatten, dropout, and dense layers. They conducted experiments on a dataset of CXR images with seven classes (COVID-19, normal, viral pneumonia, bacterial pneumonia, fibrosis, lung opacity, and TB). Using their developed architecture, they employed various classification schemes (i.e., binary, three-class, four-class, five-class, six-class, and seven-class). They compared their methodology with pre-trained VGG-16, VGG-19, and Inception-v3 models. Consequently, they proved that their model outperformed the state-of-the-art models. However, they stated that the performance of binary classification (Normal vs COVID-19) is subpar in comparison to the literature. They also mentioned that an unevenly distributed dataset affects the model's classification performance.

Emara et al. [24] developed a system that combines super-resolution methodology to enhance image details, InceptionResNetv2 to extract the features, and a multi-class support vector machine (MCSVM) to classify the extracted features. To present the model performance they used two different CXR datasets. Consequently, they achieved an accuracy of 95.80% for Dataset 1 and an accuracy of 93.45%, a sensitivity of 92.76%, a specificity of 98.58, a precision of 92.51%, and a F1-score of 90.56%, respectively for Dataset 2, containing COVID-19, lung opacity, TB, viral pneumonia and normal CXRs. Moreover, they demonstrated that using MCSVM instead of softmax layer achieves higher accuracy. Despite significant advancements in the classification of lung diseases using CXRs, current methodologies exhibit limitations in terms of generalization across diverse datasets and achieving high sensitivity alongside high specificity.

Mamalakis et al. [19] combined DenseNet121 and ResNet50 for feature extraction, yet their accuracy and sensitivity remain suboptimal at 82.9% and 69.7%, respectively. Similarly, Kim et al. [21] utilized EfficientNet v2 with additional layers but achieved only 82.20% accuracy. In contrast, Hong et al. [20] employed a multi-GAP structure with EfficientNet-B7, yielding higher accuracy but still lacking in balanced performance across all metrics. The proposed study addresses these limitations by integrating a novel hybrid model that combines advanced feature extraction techniques with a robust classification framework. Specifically, DenseNet201 is used for feature extraction, and GAP layers are employed to enhance these features. In addition to reducing the complexity of the model by minimizing the number of parameters, GAP also preserves the underlying spatial information, allowing for more effective and generalizable feature representations. Additionally, unlike previous studies, the proposed methodology incorporates the SE block as an attention mechanism, significantly boosting performance. This innovative approach results in superior accuracy, precision, and sensitivity, outperforming existing methods and providing a comprehensive, high-performing solution for multi-class lung disease classification. By leveraging the strengths of GAP, which ensures efficient feature enhancement and reduction, and SE blocks, the study fills a critical gap in the literature, demonstrating that the inclusion of an effective attention mechanism can substantially enhance model performance in medical image classification tasks.

3. Materials and Methodology

3.1. Materials

In this study, analyzes are carried out by combining data sets obtained from various sources. Table 1 displays the number of images contained within each class. Image examples from each class are given in Figure 1.

Figure 1: CXRs

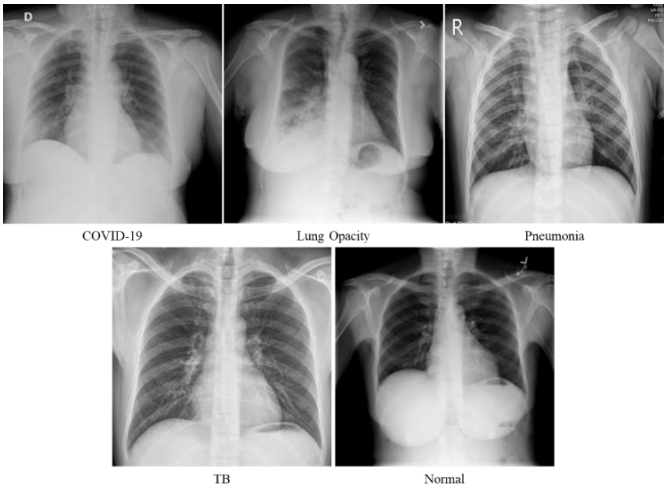

3.1.1 TB dataset

The Tuberculosis (TB) Chest Radiograph Database was compiled in a collaborative study between researchers from Qatar University in Doha, Qatar, and the University of Dhaka, Bangladesh, and colleagues in Malaysia, together with Hamad Medical Corporation and medical practitioners from Bangladesh. This dataset consists of 3500 normal, 3500 TB radiographs [25]. The dataset in question is available at the National Library of Medicine (NLM), National Institute of Allergy and Infectious

Diseases, Ministry of Health, Republic of Belarus, and NIAID TB portal. Part of this dataset (700 images) is open access, but to obtain the whole data a data sharing agreement has been signed [26].

3.1.2 Pneumonia dataset

Pneumonia CXRs were taken from Kaggle [27]. Diagnoses for these images were made by two expert physicians before being used for training a classification model. The set was also checked by a third expert to account for any rating errors. In this study, only viral pneumonia images were taken from this dataset.

3.1.3 COVID-19 dataset

The COVID-19 Radiography Database, an open-access dataset, was created by a team of researchers from Qatar University, Doha, Qatar, and University of Dhaka, Bangladesh, as well as collaborators from Pakistan and Malaysia [28], [29]. The dataset consists of four classes: COVID-19, viral pneumonia, lung opacity (i.e., non-COVID-19 lung infection), and normal.

Table 1: The combined dataset used in this study

	Train	Validation	Test	Total
Covid-19	2604	289	723	3616
TB	2520	280	700	3500
Pneumonia	1075	119	299	1493
Lung Opacity	4329	481	1202	6012
Normal	7339	815	2038	10192
Total	17867	1984	4962	24813

In this study, the dataset is divided into training and testing set with 80:20 split. Furthermore, to overcome overfitting 10% of the training set is used as a validation set. A random shuffle method is adapted while splitting the dataset.

3.2. Methods

In this work, we propose an algorithm based on DenseNet201 and SE. The architecture of the algorithm is given in Figure 2. The algorithm uses DenseNet201 as its backbone model to extract representative features. These features are then processed by the SE block to highlight important features and suppress unimportant ones. In parallel, the GAP block is used to suppress less discriminative features obtained from DenseNet201. The features from both SE and GAP are combined, using horizontal concatenation, and the resulting features are passed through a dense layer. Finally, the desired final predictions, namely class labels, are obtained.

Figure 2: Proposed model

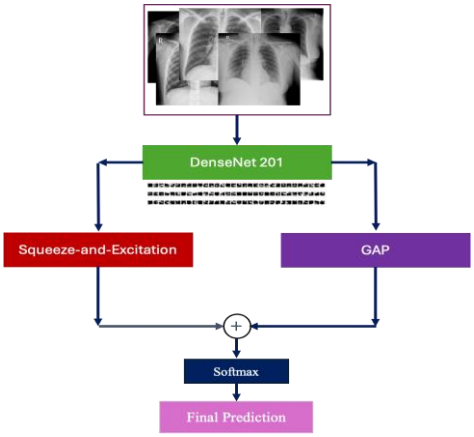

3.2.1 DenseNet201

DL networks known as CNNs excel in extracting representative features from images, which makes them preferred for disease detection and classification. These networks have a feed-forward architecture consisting of various layers, including convolutional layers for extracting local features, pooling layers for downsampling to reduce complexity and prevent overfitting, and fully connected (FC) layers for the final classification [30], [31]. Moreover, their ability to understand hidden features in images has generated significant interest in healthcare applications [23].

Despite the extraordinary performance of CNNs, their training requires very large datasets to achieve successful results, which can be challenging. In order to mitigate this limitation and enhance the generalization ability of CNNs even when datasets are limited, TL approach is often employed [32], [33]. State-of-the-art pre-trained networks such as DenseNet201, Inceptionv3, and Mobilenet, which are trained on ImageNet, are frequently used for feature extraction and image classification, notably in healthcare applications. Hence, in the proposed approach, DenseNet201, pre-trained on ImageNet, has been selected due to its proven efficacy in previous studies involving CXRs [34]–[36].

Huang et al. introduced a DL model consisting of 201 convolution layers, namely DenseNet201, in 2018 with the aim of maximizing information flow between layers [37]. This architecture incorporates multiple dense blocks, where each layer concatenates inputs from preceding layers with their respective feature maps, forwarding the concatenation to subsequent layers. This mechanism effectively prevents overfitting, particularly in scenarios with smaller training datasets.

In this study, pre-trained DenseNet201 is employed as the feature extractor. The extracted feature map obtained from the last convolution layer of DenseNet201 is fed into the SE and GAP blocks simultaneously.

3.2.2 Squeeze-and-Excitation Block

Hu et al. proposed the SE block for focusing on the channel relationship rather than spatial encodings [38]. The SE block adaptively adjusts channel-wise feature responses by explicitly modeling interdependencies among channels. When SE blocks integrated into CNNs, they highlight the important features and suppress the redundant ones, thus, increase the performance of the classification model.

In SE block, the features are initially passed through a squeeze operation, where global average pooling is applied over the spatial dimensions of each channel (input tensor). In this manner, a channel descriptor is produced, enabling the information from the global receptive field of the network to be utilized by all its layers. Then in the excitation phase, the vector obtained from the squeeze phase is fed into a feed-forward neural network in order to effectively capture channel-wise dependencies. Lastly, obtained weights from the excitation phase and the input tensor are multiplied for the aim of suppressing the redundant features and also boosting the important ones [38], [39].

In the proposed approach, the output of DenseNet201 is fed to SE block.

3.2.3 Global Average Pooling

Global average pooling blocks are designed to substitute the FC layers in the conventional CNN networks. Rather than FC layers, GAP blocks take into account the average of each feature map and output a single-dimensioned vector that can fed directly into a dense layer. For instance, considering a feature map with dimension hxwxd, the average of all h and w values are calculated and as a result, a vector with dimension 1x1xd is obtained. One of the most important advantages of GAP is its greater compatibility with the convolutional framework, as it facilitates similarities between feature maps and categories. Moreover, since there is no parameter to optimize in GAP, overfitting is avoided.

Additionally, due to GAP's ability to summarize spatial information, it is more efficient in spatially resizing the input [40], [41].

In the proposed approach, the output of DenseNet201 is fed to GAP block in parallel to SE block.

3.2.4 Concatenation and Classification

The outputs of the GAP block and the SE block are concatenated to capture the most important features. Following this concatenation, a softmax layer is applied to the combined features. Subsequently, final predictions are obtained.

3.3. Network Implementation and Training Process

Before the training, all images are resized to 224x224 pixels, which is the acceptable dimension for DenseNet201. Then, the pixels are normalized by dividing all pixel values by the largest pixel value (255). Furthermore, image augmentation techniques, including rotation (20°) and zooming (0.1), are exclusively applied to the training data. This strategy helps alleviate potential overfitting concerns associated with dataset size. To train the model, a Stochastic Gradient Descent optimizer with an initial learning rate (LR) of 0.01 is adapted. To expedite convergence, an adaptive LR decay algorithm, namely ReduceLROnPlateau, is employed. Specifically, ReduceLROnPlateau reduces the LR by a factor of 0.7 if the validation loss stagnates for 3 consecutive epochs. The categorical cross-entropy is chosen as the loss function. All experiments are carried out on the Google Colab Pro platform, providing an NVIDIA Tesla V100 GPU with Tensorflow as the backend. The model is trained for 50 epochs, and the tests are made using the model weights that provide the best validation accuracy.

3.4. Performance evaluation

The performance of the proposed algorithm is measured using accuracy, precision, recall (sensitivity), specificity, and F1-score [42], [43]. Additionally, the receiver operating characteristic curve (ROC) is utilized to evaluate the model's ability to differentiate between classes, with the AUC value serving as an output indicative of the model's performance in this regard.

4. Experimental Results

As mentioned in earlier sections, the model's performance is evaluated using the unseen test set. The results for each class and the confusion matrix are shown in Table 2 and Figure 3., respectively.

Table 2: Test results

	Accuracy (%)	Precision (%)	Recall (%)	F1- score (%)	AUC
Covid-19	99,78	99,31	99,17	99,24	1
Lung Opacity	97,56	96,39	93,43	94,89	0,99
Normal	97,46	96,05	97,84	96,94	0,99
TB	99,96	100,00	99,71	99,86	1
Pneumonia	99,96	99,34	100,00	99,67	1
Average	**98,94**	**98,22**	**98,03**	**98,12**	0,996

Figure 3: Confusion matrix of the proposed model

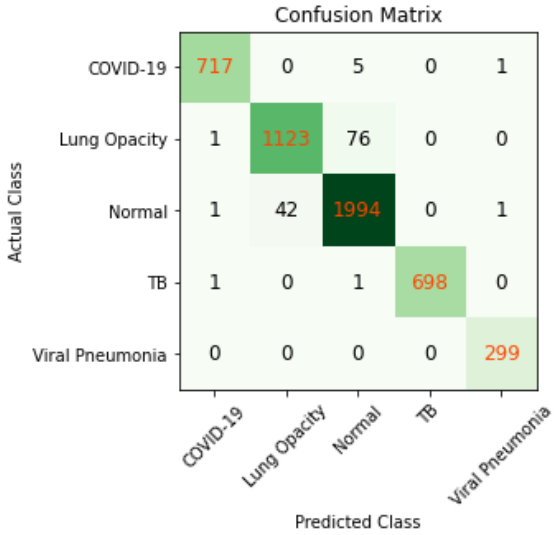

Table 2 shows that the proposed model has an average test accuracy of 98.94%, with accuracies ranging between 97.46% and 99.96% for each class. The confusion matrix reveals that the model successfully classified pneumonia and TB cases but misclassified five COVID-19 images as normal and one COVID-19 as pneumonia, respectively. It also shows that the classes most often confused were lung opacity and normal images. Despite this, the overall accuracy is promising. The reason for this confusion is the severity of lung opacity. When the opacity is mild, the images can look similar to normal CXRs. Since the dataset does not include information about the severity of conditions, it is hard to evaluate this issue accurately. The ROC curve, shown in Figure 4, indicates that the AUC values for COVID-19, pneumonia, and TB are 1.00, while the AUC values for normal and lung opacity are 0.99, resulting in a micro-average of 1.0.

Figure 4: ROC curve of the proposed model

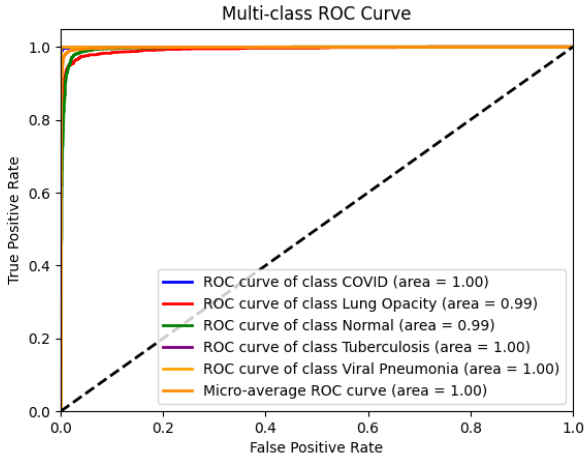

5. Ablation studies

In this study, to express the effectiveness of the proposed model, ablation studies are performed. The dataset is trained and tested with Densenet201, Densenet201+SE block, and Densenet201+GAP block, respectively. Table 3 shows the results of these different models. As seen in Table 3, SE blocks improve

the performance of transfer learning models i.e. DenseNet201. Additionally, applying GAP rather than FC layer boosts performance by approximately 5% in accuracy. Finally, it is evident that the proposed methodology which combines both SE and GAP enhances the model's classification performance and results the higher accuracy as well as precision, recall, and F1-score.

Table 3: Results of ablation studies

Model	Accuracy (%)	Precision (%)	Recall (%)	F1- score (%)
Densenet+FC	95,58	90,57	89,36	89,93
Densenet+SE	98,73	97,50	97,58	97,54
Densenet+GAP	98,90	98,02	97,79	97,90
Proposed model	98,94	98,22	98,03	98,12

6. Grad-Cam

To improve the interpretability of the model, this study uses the Gradient-Weighted Class Activation Maps (Grad-CAM) algorithm. The Grad-CAMs are powerful tools for interpreting the decisions made by CNNs. These maps provide a visual representation of the regions within the image that the model focuses on when making predictions. The Grad-CAM process starts by feeding the image into the model and then calculating the gradient of the output score for a specific target class based on the activations in the final CNN layer. These gradients show how much each pixel contributes to the class prediction. Next, they are converted to neuron importance weights using global max pooling [44]. After that, a weighted combination of the activation maps is created using these weights, resulting in a heatmap. This heatmap is then directly applied to the original image to highlight the image regions crucial for class prediction [45]. Examples of Grad-CAMs for each class are shown in Figure 5.

Figure 5: Grad-CAM visualization

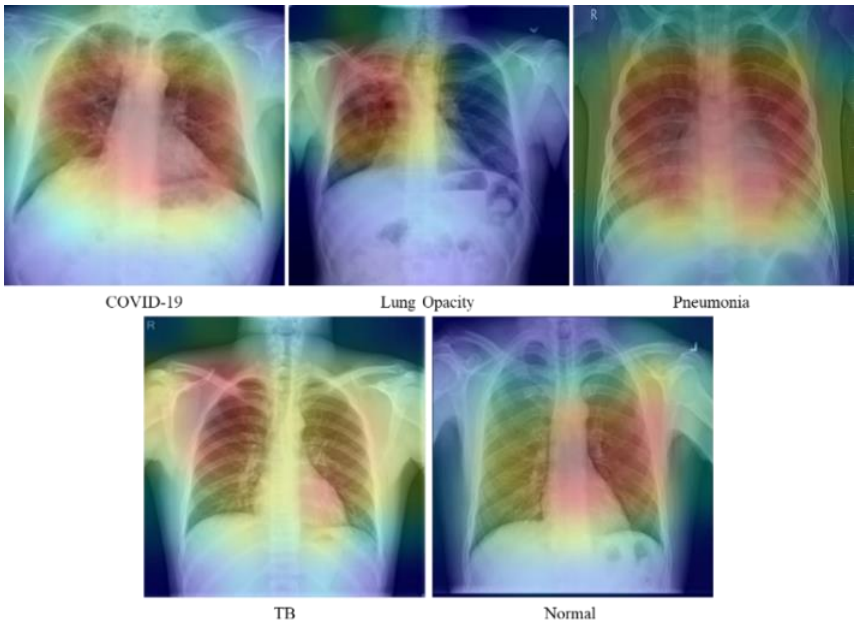

In Figure 5, a jet color scheme is used to colorize the heatmaps. Blue represents the negligible values for classification. Yellow and green represent moderate values, indicating a relatively lower degree of

feature extraction. In contrast, red and dark red represent higher values, suggesting that the features within those regions represent the specific class [46]. Therefore, Fig 4 helps us to pinpoint the key areas in the example CXRs, where the distinctive features that differentiate the five classes are most noticeable.

7. Discussion

In this study, we propose a method that combines both GAP and SE attention mechanisms, along with a TL approach. For training and testing the proposed algorithm, we used a dataset, created from three public datasets. Additionally, this method does not require hand-crafted features or preprocessing. We demonstrated that our approach can extract representative features and achieve high performance in image classification.

Table 4 presents various DL approaches for classifying five-class CXRs, which include TB, pneumonia, and COVID-19. However, it is clear that making a one-to-one comparison is not feasible due to differences in dataset splits and data sizes.

Despite this, our proposed method clearly outperforms all other studies that utilized used utilizing five-class classification, including COVID-19, TB, and pneumonia, presented.

Table 4: Comparison of the proposed methodology with literature

	Accuracy (%)	Precision (%)	Recall (Sensitivity) (%)	F1- score (%)	Specificity (%)
2020, Oh et al. [33]	88.9	83.4	85.9	84.4	96.4
2021, Xu et al. [47]	97.06	97	97	97	
2022, Naseem et al. [48]	94.666	94.827	94.666		98.666
2022, Sharma et al. [18]	95.05	95.40	95.05	95.19	
2022, Yi et al. [49]	91.796	92.062	91.796	91.892	
2023, Emara et al. [24]	93.45	92.51	92.76	90.56	98.58
2023, Indumathi et al. [50]	98.71	98.78	97.82	98,38	
2023, Oh et al. [51]	97.72		95.93		99.05
2023, Sultana et al. [23]	96.96	95	96	95	
2023, Hamza et al. [52]	97.2	96.94	96.88	96.60	
2024, Proposed meth-odology	**98,94**	**98,22**	**98,03**	**98,12**	**99.18**

8. Conclusion and Future Works

Pulmonary diseases such as COVID-19, pneumonia, and TB are contagious and have become major causes of death recently. Early and accurate diagnosis is crucial for managing the progression of these diseases and preventing serious complications. CXRs are the most common diagnostic imaging technique because they are available, easy to use, have low radiation exposure, and are affordable. However, manual inspection of CXRs depends on the radiologist and therefore, is prone to inter-/intra-personal observation mistakes. Because of these challenges, DL approaches for detecting and classifying diseases from CXRs have gained attention from researchers in recent years.

In this study, we propose a robust DL approach for the classification and detection of various lung diseases, including TB, pneumonia, COVID-19, and lung opacity. DenseNet201 is used as the backbone of the proposed model for extracting representative features and an attention mechanism, SE, is utilized with GAP. In conclusion, the synergistic application of DenseNet201, GAP, and SE mechanisms enhances the model's performance, generalization ability, and interpretability, leading to an effective and reliable classification model. Thus, a methodology that is appropriate for lung disease classification is proposed. Furthermore, we have also provided a visual representation of the proposed model's decision-making process using Grad-CAM. Since this approach effectively removes the "black box" mystery of the model and makes the decision more transparent and interpretable, radiologists can leverage these visualizations to gain a deeper understanding of the model's reasoning, promoting greater trust and facilitating its integration into their clinical practice.

9. References

1. Zainab Yousuf Zaidi S, Usman Akram M, Jameel A, Alghamdi NS. Lung Segmentation-Based Pulmonary Disease Classification Using Deep Neural Networks. *IEEE Access*. 2021;9:125202-125214. doi:10.1109/ACCESS.2021.3110904
2. Ho TKK, Gwak J. Utilizing Knowledge Distillation in Deep Learning for Classification of Chest X-Ray Abnormalities. *IEEE Access*. 2020;8:160749-160761. doi:10.1109/ACCESS.2020.3020802
3. Bhandari M, Shahi TB, Siku B, Neupane A. Explanatory classification of CXR images into COVID-19, Pneumonia and Tuberculosis using deep learning and XAI. *Comput Biol Med*. 2022;150(June):106156. doi:10.1016/j.compbiomed.2022.106156
4. Malik H, Anees T, Din M, Naeem A. CDC_Net: multi-classification convolutional neural network model for detection of COVID-19, pneumothorax, pneumonia, lung Cancer, and tuberculosis using chest X-rays. *Multimed Tools Appl*. Published online April 1, 2022. doi:10.1007/s11042-022-13843-7
5. Zotin A, Hamad Y, Simonov K, Kurako M. Lung boundary detection for chest X-ray images classification based on GLCM and probabilistic neural networks. In: *Procedia Computer Science*. Vol 159. Elsevier B.V.; 2019:1439-1448. doi:10.1016/j.procs.2019.09.314
6. Souza JC, Bandeira Diniz JO, Ferreira JL, França da Silva GL, Corrêa Silva A, de Paiva AC. An automatic method for lung segmentation and reconstruction in chest X-ray using deep neural networks. *Comput Methods Programs Biomed*. 2019;177:285-296. doi:10.1016/j.cmpb.2019.06.005
7. Agrawal T, Choudhary P. Segmentation and classification on chest radiography: a systematic survey. *Vis Comput*. Published online 2022. doi:10.1007/s00371-021-02352-7
8. Li F, Shi JX, Yan L, et al. Lesion-aware convolutional neural network for chest radiograph classification. *Clin Radiol*. 2021;76(2):155.e1-155.e14. doi:10.1016/j.crad.2020.08.027
9. Fang J, Xu Y, Zhao Y, Yan Y, Liu J, Liu J. Weighing features of lung and heart regions for thoracic disease classification. *BMC Med Imaging*. 2021;21(1). doi:10.1186/s12880-021-00627-y
10. Wang K, Zhang X, Huang S, Chen F, Zhang X, Huangfu L. Learning to Recognize Thoracic Disease in Chest X-Rays with Knowledge-Guided Deep Zoom Neural Networks. *IEEE Access*. 2020;8:159790-159805. doi:10.1109/ACCESS.2020.3020579
11. Munawar F, Azmat S, Iqbal T, Gronlund C, Ali H. Segmentation of Lungs in Chest X-Ray Image Using Generative Adversarial Networks. *IEEE Access*. 2020;8:153535-153545. doi:10.1109/ACCESS.2020.3017915

12. Sogancioglu E, Çallı E, van Ginneken B, et al. *Deep Learning for Chest X-Ray Analysis: A Survey*. Vol 72. Elsevier B.V.; 2021:102125. doi:10.1016/j.media.2021.102125
13. Gopatoti A, Vijayalakshmi P. Optimized chest X-ray image semantic segmentation networks for COVID-19 early detection. *J Xray Sci Technol*. 2022;30(3):491-512. doi:10.3233/XST-211113
14. Bashar A, Latif G, Brahim G Ben, Mohammad N, Alghazo J. COVID-19 pneumonia detection using optimized deep learning techniques. *Diagnostics*. 2021;11(11). doi:10.3390/diagnostics11111972
15. Azad AK, Mahabub-A-Alahi, Ahmed I, Ahmed MU. In Search of an Efficient and Reliable Deep Learning Model for Identification of COVID-19 Infection from Chest X-ray Images. *Diagnostics*. 2023;13(3). doi:10.3390/diagnostics13030574
16. Ahmad M, Bajwa UI, Mehmood Y, Anwar MW. Lightweight ResGRU: a deep learning-based prediction of SARS-CoV-2 (COVID-19) and its severity classification using multimodal chest radiography images. *Neural Comput Appl*. Published online 2023. doi:10.1007/s00521-023-08200-0
17. Brima Y, Atemkeng M, Djiokap ST, Ebiele J, Tchakounté F. Transfer learning for the detection and diagnosis of types of pneumonia including pneumonia induced by COVID-19 from chest X-ray images. *Diagnostics*. 2021;11(8). doi:10.3390/diagnostics11081480
18. Sharma A, Mishra PK. Covid-MANet: Multi-task attention network for explainable diagnosis and severity assessment of COVID-19 from CXR images. *Pattern Recognit*. 2022;131. doi:10.1016/j.patcog.2022.108826
19. Mamalakis M, Swift AJ, Vorselaars B, et al. DenResCov-19: A deep transfer learning network for robust automatic classification of COVID-19, pneumonia, and tuberculosis from X-rays. *Comput Med Imaging Graph*. 2021;94(September):102008. doi:10.1016/j.compmedimag.2021.102008
20. Hong M, Rim B, Lee HC, Jang HU, Oh J, Choi S. Multi-class classification of lung diseases using cnn models. *Appl Sci*. 2021;11(19):1-17. doi:10.3390/app11199289
21. Kim S, Rim B, Choi S, Lee A, Min S, Hong M. Deep Learning in Multi-Class Lung Diseases' Classification on Chest X-ray Images. *Diagnostics*. 2022;12(4). doi:10.3390/diagnostics12040915
22. Iqbal A, Usman M, Ahmed Z. Tuberculosis chest X-ray detection using CNN-based hybrid segmentation and classification approach. *Biomed Signal Process Control*. 2023;84(July 2022):104667. doi:10.1016/j.bspc.2023.104667
23. Sultana A, Nahiduzzaman M, Bakchy SC, et al. A Real Time Method for Distinguishing COVID-19 Utilizing 2D-CNN and Transfer Learning. *Sensors*. 2023;23(9). doi:10.3390/s23094458
24. Emara HM, Shoaib MR, El-Shafai W, et al. Simultaneous Super-Resolution and Classification of Lung Disease Scans. *Diagnostics*. 2023;13(7):1-28. doi:10.3390/diagnostics13071319
25. Rahman T, Khandakar A, Kadir MA, et al. Reliable tuberculosis detection using chest X-ray with deep learning, segmentation and visualization. *IEEE Access*. 2020;8:191586-191601. doi:10.1109/ACCESS.2020.3031384
26. (NIH) NI of H. Tuberculosis (TB) data science for public health impact. https://tbportals.niaid.nih.gov/download-data
27. Mooney P. Chest X-Ray Images (Pneumonia). https://www.kaggle.com/datasets/paultimothymooney/chest-xray-pneumonia/data
28. Chowdhury MEH, Rahman T, Khandakar A, et al. Can AI Help in Screening Viral and COVID-19 Pneumonia? *IEEE Access*. 2020;8:132665-132676. doi:10.1109/ACCESS.2020.3010287
29. Rahman T, Khandakar A, Qiblawey Y, et al. Exploring the effect of image enhancement techniques

on COVID-19 detection using chest X-ray images. *Comput Biol Med*. 2021;132(November):104319. doi:10.1016/j.compbiomed.2021.104319
30. Salini Y, HariKiran J. ViT: Quantifying Chest X-Ray Images Using Vision Transformer & XAI Technique. *SN Comput Sci*. 2023;4(6). doi:10.1007/s42979-023-02204-2
31. Oltu B, Guney S, Dengiz B, Agildere M. Automated Tuberculosis Detection Using Pre-Trained CNN and SVM. In: *2021 44th International Conference on Telecommunications and Signal Processing, TSP 2021*. ; 2021. doi:10.1109/TSP52935.2021.9522644
32. Shrivastava VK, Pradhan MK. Diagnosis of COVID-19 based on chest X-ray images using pre-trained deep convolutional neural networks. *Intell Decis Technol*. 2022;16(1):169-180. doi:10.3233/IDT-210002
33. Oh Y, Park S, Ye JC. Deep Learning COVID-19 Features on CXR Using Limited Training Data Sets. *IEEE Trans Med Imaging*. 2020;39(8):2688-2700. doi:10.1109/TMI.2020.2993291
34. Ukwuoma CC, Qin Z, Agbesi VK, et al. LCSB-inception: Reliable and effective light-chroma separated branches for Covid-19 detection from chest X-ray images. *Comput Biol Med*. 2022;150. doi:10.1016/j.compbiomed.2022.106195
35. Lee CP, Lim KM. COVID-19 Diagnosis on Chest Radiographs with Enhanced Deep Neural Networks. *Diagnostics*. 2022;12(8). doi:10.3390/diagnostics12081828
36. Chutia U, Shanker A, Jyoti T, Singh P, Kumar V. Classification of Lung Diseases Using an Attention - Based Modified DenseNet Model. 2024;(0123456789). doi:10.1007/s10278-024-01005-0
37. Huang G, Liu Z, van der Maaten L, Weinberger KQ. Densely Connected Convolutional Networks. Published online August 24, 2016. http://arxiv.org/abs/1608.06993
38. Hu J, Shen L, Albanie S, Sun G, Wu E. Squeeze-and-Excitation Networks. Published online September 5, 2017. http://arxiv.org/abs/1709.01507
39. Dey S, Bhattacharya R, Malakar S, Schwenker F, Sarkar R. CovidConvLSTM: A fuzzy ensemble model for COVID-19 detection from chest X-rays[Formula presented]. *Expert Syst Appl*. 2022;206. doi:10.1016/j.eswa.2022.117812
40. Lin M, Chen Q, Yan S. Network in network. *2nd Int Conf Learn Represent ICLR 2014 - Conf Track Proc*. Published online 2014:1-10.
41. Nayak SR, Nayak J, Sinha U, Arora V, Ghosh U, Satapathy SC. An Automated Lightweight Deep Neural Network for Diagnosis of COVID-19 from Chest X-ray Images. *Arab J Sci Eng*. Published online 2021. doi:10.1007/s13369-021-05956-2
42. Oltu B, Akşahin MF, Kibaroğlu S. A novel electroencephalography based approach for Alzheimer's disease and mild cognitive impairment detection. *Biomed Signal Process Control*. 2021;63. doi:10.1016/j.bspc.2020.102223
43. Hassanlou L, Meshgini S, Afrouzian R, Farzamnia A, Moung EG. FirecovNet: A Novel, Lightweight, and Fast Deep Learning-Based Network for Detecting COVID-19 Patients Using Chest X-rays. *Electron*. 2022;11(19). doi:10.3390/electronics11193068
44. Wang B, Zhang W. MARnet: Multi-scale adaptive residual neural network for chest X-ray images recognition of lung diseases. *Math Biosci Eng*. 2022;19(1):331-350. doi:10.3934/mbe.2022017
45. Choudhary P, Hazra A. Chest disease radiography in twofold: using convolutional neural networks and transfer learning. *Evol Syst*. 2021;12(2):567-579. doi:10.1007/s12530-019-09316-2
46. Umair M, Khan MS, Ahmed F, et al. Detection of COVID-19 using transfer learning and grad-cam

visualization on indigenously collected X-ray dataset. *Sensors*. 2021;21(17). doi:10.3390/s21175813
47. Xu Y, Lam HK, Jia G. MANet: A two-stage deep learning method for classification of COVID-19 from Chest X-ray images. *Neurocomputing*. 2021;443:96-105. doi:10.1016/j.neucom.2021.03.034
48. Naseem MT, Hussain T, Lee CS, Khan MA. Classification and Detection of COVID-19 and Other Chest-Related Diseases Using Transfer Learning. *Sensors*. 2022;22(20). doi:10.3390/s22207977
49. Yi SL, Qin SL, She FR, Wang TW. RED-CNN: The Multi-Classification Network for Pulmonary Diseases. *Electron*. 2022;11(18). doi:10.3390/electronics11182896
50. Indumathi V, Siva R. An efficient lung disease classification from X-ray images using hybrid Mask-RCNN and BiDLSTM. *Biomed Signal Process Control*. 2023;81. doi:10.1016/j.bspc.2022.104340
51. Oh J, Park C, Lee H, et al. OView-AI Supporter for Classifying Pneumonia, Pneumothorax, Tuberculosis, Lung Cancer Chest X-ray Images Using Multi-Stage Superpixels Classification. *Diagnostics*. 2023;13(9):1-16. doi:10.3390/diagnostics13091519
52. Hamza A, Khan MA, Alhaisoni M, et al. D2BOF-COVIDNet: A Framework of Deep Bayesian Optimization and Fusion-Assisted Optimal Deep Features for COVID-19 Classification Using Chest X-ray and MRI Scans. *Diagnostics*. 2023;13(1). doi:10.3390/diagnostics13010101